Nigerian Journal of Physics (NJP)

ISSN: 1595-0611

Volume 32(1), March 2023

Energy Spectra of Shifted Screened Kratzer Potential (SSKP) for some Diatomic Molecules in the Presence of Magnetic and Aharonov-Bohm Flux Fields using Extended Nikiforov-Uvarov Method

***[1]Ibrahim, N., [2]Izam, M. M., [2]Jabil, Y. Y.**

[1]Department of Physics, University of Maiduguri, Maiduguri Nigeria
[2]Department of Physics, University of Jos, Jos Nigeria

*Corresponding author's email: nuhuphysics@unimaid.edu.ng

ABSTRACT

It is well-established in the literature that some magnetic field-related phenomena, such as Zeeman effect, have recently become particular significant in changing the behavior of some quantum system. Notably, degeneracy is eleiminated by the magnetic field. It has also recently been found that the Aharonov-Bohm (AB)-flux field serves this purpose when it is introduced to a quantum system. Therefore, in this research work, the effect of shifting parameters on the energy spectra of Hydrogen (H_2), Lithium Hydride (LiH), Hydrogen Chloride (HCl), and Carbon (II) oxide (CO) diatomic molecules with shifted screened Kratzer potential model in the presence of magnetic and Aharonov-Bohm (AB)-flux fields are investigated using Extended Nikiforov-Uvarov (ENU) method. We obtained the energy equation in a closed form and its corresponding wave function in terms of hypergeometric polynomials respectively. The obtained energy equation are used to study the selected diatomic molecules. It is observed that the effect of shifting parameters influences the energy eigenvalues of diatomic molecules to becomes strongly negative or bound. From our finding, it could be concluded that to regulate the energy spectra of these diatomic molecules, the shifting parameters will do so greatly. This is because it has been established that, potential energy functions with more parameters are better than those with fewer parameters as they tend to fit experimental data. It is also seen that the presence of magnetic and Aharonov-Bohm (AB)-flux fields breaks degeneracy in the energy levels of diatomic molecules. As a special case, when the shifting parameters in the shifted screened Kratzer potential is set to zero, then the well-known Kratzer potential and screened Kratzer potential are recovered. Numerical results for the energy eigenvalues are also obtained for different quantum states. Our results are seen to agree with the results in literature.

Keywords:
Diatomic molecules,
Extended Nikiforov-Uvarov (ENU) method,
Magnetic and AB-flux fields,
Schrodinger Equation (SE),
Shifted Screened Kratzer Potential (SSKP).

INTRODUCTION

Calculating the energy eigenvalue and eigenfunction of diatomic molecules has attracted a lot of attention in some years back across many fields of physics, Bayrak et al. (2006). In the literature, numerous researchers have developed much interest over the years towards finding the solutions of relativistic and non-relativistic wave equations for different potential models. These include Deng–Fan Potential (Edet et al., 2022), Improved Ultra-Generalized Exponential Hyperbolic Potential (Ikot et al., 2021), Inverse Quadratic Yukawa Potential (Horchani et al., 2021), Modified Kratzer Potential (Onyenegecha et al., 2021), Screened Kratzer Potential (Ikot et al., 2020), Pseudoharmonic Potential (Ikot et al., 2020), Improved Kratzer Potential (Rampho et al., 2020), Kratzer Potential (Aygun et al., 2012), Manning-Rosen Potential (Hassanabadi et al., 2012; Ikhdair, 2012).

Also, several researchers have used a variety of methods to obtain the solutions of the relativistic and non-relativistic wave equations using a chosen potential model. These methods include the Nikiforov-Uvarov (NU) method (Nikiforov & Uvarov, 1988), Nikiforov-Uvarov-Functional Analysis (NUFA) method (Ikot et al., 2021), Extended Nikiforov-Uvarov (ENU) method (Karayer et al., 2015), parametric NU method (Tezcan & Sever, 2009), formula method (Falaye et al., 2014), Proper Quantization Rule (PQR) method (Serrano et al., 2010).

In most of the recent studies, there are many researchers in the literature that considered the influence of magnetic and Aharonov-Bohm (AB)-flux fields on quantum systems. For example, Aygun et al. (2012) obtained energy eigensolution of the Kratzer potential with and without the influence of an induced constant magnetic field for 2D Schrödinger equation using the asymptotic iteration method (Eshghi & Mehraban, 2017). Under the radial scalar power potential, had studied particle confined by a magnetic and Aharonov-Bohm (AB)-flux fields. Ikhdair et al. (2012), (Ikhdair & Hamzavi, 2012) had studied 2D harmonic and pseudo-harmonic oscillators in the presence of external fields and calculate the energy spectrum and wave function of an electron. Khordad, (2010a & 2010b) and Cetin, (2008) examined various spectral properties of a charged particle confined by a harmonic oscillator under the effect of the external strong magnetic field and Aharonov-Bohm (AB) flux field produced by a solenoid and obtained the eigensolution. Ferkous & Bounames, (2013) has solved the 2D Pauli equation plus Hulthen potential for spin-1/2 particle under the influence of AB flux field. Ferkous et al. (2019) studied the interaction between spin and magnetic flux and obtained bound-state energy eigenvalues for a spin-1/2 particle subjected to the modified Pöschl-Teller potential in the presence of Aharonov-Bohm field.

Thus, the present research work, intends to investigate the effect of the Shifted Screened-Kratzer Potential (SSKP) model on the energy spectra of some selected diatomic molecules in the presence of magnetic and Aharonov-Bohm (AB) flux fields which has not been studied elsewhwere. The SSKP model (Ibrahim et al. 2022) is given by

$$V(r) = -2D_e\left(\frac{a}{r}-\frac{b}{2r^2}\right)(2\lambda+\gamma e^{-\alpha r}) \qquad (1)$$

where D_e is the dissociation energy, $a = r_e, b = r_e^2, r_e$ being the equilibrium bond length, α is the screening parameter, λandγ are constants called 'shifting parameters', and they can be adjusted as desired.

MATERIAL AND METHODS

The Extended Nikiforov-Uvarov (ENU) method is an extension of Nikiforov-Uvarov method for solving any second-order linear differential equation which has at most four singular points (Karayer *et al.*, 2015): The ENU method is given in the form:

$$\psi_e''(s) + \frac{\tilde{\tau}_e(s)}{\sigma_e(s)}\psi_e'(s) + \frac{\tilde{\sigma}_e(s)}{\sigma_e^2(s)}\psi_e(s) = 0 \qquad (2)$$

where $\tilde{\tau}_e(s)$, $\sigma_e(s)$ and $\tilde{\sigma}_e(s)$ are polynomials of at most second, third and fourth degrees respectively. Equation (2) is called the basic equation of the ENU method. The subscript $e$stands for "extended". To find the particular solution of Equation (2), we use the following transformation:

$$\psi_e(s) = \phi_e(s)y_e(s) \qquad (3)$$

which then reduces Equation (2) to an equation of hypergeometric-type equation,

$$\sigma_e(s)y_e'' + \tau_e(s)y_e' + h(s)y_e = 0 \qquad (4)$$

where

$$h(s) = h_n(s) = -\frac{n}{2}\tau_e'(s) - \frac{n(n-1)}{6}\sigma_e''(s) + C_n, \quad n = 0,1,2,\ldots, \qquad (5)$$

where C_n are integrating constants and $\tau_e(s)$ is defined as:

$$\tau_e(s) = \tilde{\tau}_e(s) + 2\pi_e(s) \qquad (6)$$

which must have a negative derivative. Equation (4) has polynomial solutions $y_e(s)$ that are given by the Rodrigues relation

$$y_n(s) = \frac{B_n}{\rho(s)}\frac{d^n}{ds^n}[\sigma^n(s)\rho(s)] \qquad (7)$$

where B_n is the normalization constant and $\rho(s)$ is called the density or weight function and must satisfy the condition

$$(\sigma\rho)' = \tau\rho \qquad (8)$$

The function $\phi_e(s)$ satisfies

$$\frac{\phi_e'(s)}{\phi_e(s) = \frac{\pi_e(s)}{\sigma_e(s)}} \qquad (9)$$

where $\pi_e(s)$ and the parameter $h(s)$are defined as:

$$\pi_e(s) = \frac{\sigma_e'(s) - \tilde{\tau}_e(s)}{2} \pm \sqrt{\left(\frac{\sigma_e'(s) - \tilde{\tau}_e(s)}{2}\right)^2 - \tilde{\sigma}_e(s) + G(s)\sigma_e(s)} \qquad (10)$$

and

$$h(s) - \pi_e'(s) = g(s) \qquad (11)$$

Here, the function $\pi_e(s)$ is a polynomial of second degree unlike the conventional NU method that has a polynomial of first degree. Based on the ENU method, the determination of $G(s)$ is crucial in finding $\pi_e(s)$. It is determine by requiring the expression under the square root in Equation (10) to be a square of the second degree polynomial.

Equating Equation (5) and Equation (11), we obtain the energy eigenvalue equation and for the eigenfunction equation can be acquired as follows: the functions $\phi_e(s)$ and $\rho_e(s)$ are calculated from Equation (8) and Equation (9) and substituting their values into Equation (3), then the eigenfunction equation can be obtained.

Schrodinger Equation of the SSKP with Magnetic and AB Fields

A generalized form of the Schrodinger Equation (SE) for a charged particle moving under the influence of the vector potential $\vec{A}$ is written as (Purohit et al., 2020; Rampho et al., 2020; Ikot et al., 2020; 2021):

$$\left(\vec{p} + \frac{e}{c}\vec{A}\right)^2 \psi(r,\phi) = 2\mu[E_{nm} - V(r)]\psi(r,\phi) \qquad (12)$$

where e and μ are the charge of the particle and reduced mass of the system respectively, E_{nm} is the energy eigenvalues, vector momentum $\vec{p} = -i\hbar\vec{\nabla}$, $c$is the velocity of light, vector potential and $V(r)$ scalar potential. To indicate the magnetic field and AB-flux field together, we express the vector potential $\vec{A}$ as a sum of two terms $\vec{A} = \vec{A}_{\phi_1} + \vec{A}_{\phi_2}$ having azimuthal components

$$\vec{A}_{\phi_1} = \frac{\vec{B}e^{-\alpha r}}{1-e^{-\alpha r}}\hat{\phi} \text{ and } \vec{A}_{\phi_2} = \frac{\Phi_{AB}}{2\pi r}\hat{\phi} \qquad (13)$$

where $\vec{B}$ is the applied external magnetic field with $\vec{\nabla}\times\vec{A}_{\phi_1} = \vec{B}$, $\vec{A}_{\phi_2}$ represents the additional magnetic flux Φ_{AB} created by a solenoid with $\vec{\nabla}\cdot\vec{A}_{\phi_2} = 0$. Then the vector potential can be written as:

$$\vec{A} = \left(\frac{\vec{B}e^{-\alpha r}}{1-e^{-\alpha r}} + \frac{\Phi_{AB}}{2\pi r}\right)\hat{\phi} \qquad (14)$$

where $\hat{\phi}$ is the direction of magnetic flux around the solenoid. Also, we assume a wavefunction in the cylindrical coordinates to be $\psi(r,\phi) = (2\pi r)^{-\frac{1}{2}}e^{im\phi}\chi_{nm}(r)$, where m is the magnetic quantum number. Substituting Equations. (1) and (14) into Equation (12), we have

$$\left(i\hbar\vec{\nabla} - \frac{e}{c}\vec{A}\right)^2\psi(r,\phi) = 2\mu\left[E_{nm} + 2D_e\left(\frac{a}{r} - \frac{b}{2r^2}\right)(2\lambda + \gamma e^{-\alpha r})\right]\psi(r,\phi) \qquad (15)$$

For convenience, let us introduce $\kappa = -\frac{e}{c}$, so that Equation (15) becomes

$$\left(i\hbar\vec{\nabla} + \kappa\vec{A}\right)^2\psi(r,\phi) = 2\mu\left[E_{nm} + 2D_e\left(\frac{a}{r} - \frac{b}{2r^2}\right)(2\lambda + \gamma e^{-\alpha r})\right]\psi(r,\phi)$$

$$\left(i\hbar\vec{\nabla} + \kappa\vec{A}\right)^2\psi(r,\phi) = 2\mu\left[E_{nm} + 4D_e a\lambda\frac{1}{r} - 2D_e b\lambda\frac{1}{r^2} + 2D_e a\gamma\frac{e^{-\alpha r}}{r} - D_e b\gamma\frac{e^{-\alpha r}}{r^2}\right]\psi(r,\phi) \qquad (16)$$

carrying out some algebraic calculations in Equation (16) we get the 2nd order differential equation (DE) given as follows:

$$\chi''_{nm}(r) + \begin{bmatrix} \frac{2\mu E_{nm}}{\hbar^2} + \frac{2\mu}{\hbar^2}\left(4D_e a\lambda\frac{1}{r} - 2D_e b\lambda\frac{1}{r^2} + 2D_e a\gamma\frac{e^{-\alpha r}}{r} - D_e b\gamma\frac{e^{-\alpha r}}{r^2}\right) + \frac{1}{4r^2} - \frac{m^2}{r^2} \\ + \frac{2m\kappa\vec{B}e^{-\alpha r}}{\hbar(1-e^{-\alpha r})r} + \frac{m\kappa\Phi_{AB}}{\hbar\pi r^2} - \frac{\kappa^2\vec{B}^2e^{-2\alpha r}}{\hbar^2(1-e^{-\alpha r})^2} - \frac{\kappa^2\vec{B}\Phi_{AB}e^{-\alpha r}}{\hbar^2(1-e^{-\alpha r})\pi r} - \frac{\kappa^2\Phi_{AB}^2}{4\pi^2\hbar^2r^2} \end{bmatrix}\chi_{nm}(r) = 0 \qquad (17)$$

Equation (17) is a complicated differential equation that cannot be solvable easily due to the presence of centrifugal $\frac{1}{r^2}$ as well as reciprocal $\frac{1}{r}$ terms. For analytical approximate solution with this potential for $\ell \neq 0$, we employ the Greene-Aldrich approximation scheme (Greene and Aldrich, 1976) to bypass these terms. This approximation is given by:

$$\frac{1}{r^2} \approx \frac{\alpha^2}{(1-e^{-\alpha r})^2}, \Rightarrow \frac{1}{r} \approx \frac{\alpha}{(1-e^{-\alpha r})} \qquad (18)$$

Equation (18) ceases to exist as an appropriate approximation to the centrifugal term once the screening parameter α is big because it is for a short-range potential. Consequently, the approximation is useable when $\alpha r \ll 1$. Employing the approximation term of Equation (18) into Equation (17) we have:

$$\chi''_{nm}(r) + \begin{bmatrix} \frac{2\mu E_{nm}}{\hbar^2} + \frac{8\mu\alpha D_e a\lambda}{\hbar^2(1-e^{-\alpha r})} - \frac{4\mu\alpha^2 D_e b\lambda}{\hbar^2(1-e^{-\alpha r})^2} + \frac{4\mu\alpha D_e a\gamma}{\hbar^2}\frac{e^{-\alpha r}}{(1-e^{-\alpha r})} - \frac{2\mu\alpha^2 D_e b\gamma}{\hbar^2}\frac{e^{-\alpha r}}{(1-e^{-\alpha r})^2} \\ + \frac{2m\kappa}{\hbar}\left(\frac{\alpha\vec{B}e^{-\alpha r}}{(1-e^{-\alpha r})^2}\right) - \frac{\kappa^2\vec{B}^2e^{-2\alpha r}}{\hbar^2(1-e^{-\alpha r})^2} - \frac{\kappa^2\alpha\vec{B}\Phi_{AB}e^{-\alpha r}}{\hbar^2(1-e^{-\alpha r})^2\pi} - \frac{\left[(m+\tau)^2 - \frac{1}{4}\right]\alpha^2}{(1-e^{-\alpha r})^2} \end{bmatrix}\chi_{nm}(r) = 0 \qquad (19)$$

where we have defined the following parameters as $\phi_0 = \frac{hc}{e}$ and $\tau = \frac{\Phi_{AB}}{\phi_0}$.

Now introducing the ENU method of Equation (2) into Equation (19) with the following coordinate transformation $s = e^{-\alpha r}$, we have

$$\frac{d^2\chi_{nm}(r)}{ds^2} + \frac{1}{s}\frac{d\chi_{nm}(r)}{ds} + \frac{1}{s^2}\begin{bmatrix} \frac{2\mu E_{nm}}{\hbar^2\alpha^2} + \frac{8\mu D_e a\lambda}{\hbar^2\alpha(1-s)} - \frac{4\mu D_e b\lambda}{\hbar^2(1-s)^2} + \frac{4\mu D_e a\gamma}{\hbar^2\alpha}\frac{s}{(1-s)} - \frac{2\mu D_e b\gamma}{\hbar^2}\frac{s}{(1-s)^2} \\ + \frac{2m\kappa}{\hbar}\left(\frac{\vec{B}s}{\alpha(1-s)^2}\right) - \frac{\kappa^2\vec{B}^2s^2}{\hbar^2\alpha^2(1-s)^2} - \frac{\kappa^2\vec{B}\Phi_{AB}s}{\hbar^2\alpha(1-s)^2\pi} - \frac{\left[(m+\tau)^2 - \frac{1}{4}\right]}{(1-s)^2} \end{bmatrix}\chi_{nm}(r) = 0 \qquad (20)$$

To make Equation (20) solvable with ENU method, let's introduce the following dimensionless parameters

$$\varepsilon_{nm} = -\frac{2\mu E_{nm}}{\hbar^2\alpha^2}, \delta_1 = \frac{8\mu D_e a\lambda}{\hbar^2\alpha}, \delta_2 = \frac{4\mu D_e b\lambda}{\hbar^2}, \delta_3 = \frac{4\mu D_e a\gamma}{\hbar^2\alpha},$$

$$\delta_4 = \frac{2\mu D_e b\gamma}{\hbar^2}, \delta_5 = \frac{2m\kappa\vec{B}}{\hbar\alpha}, \delta_6 = \frac{\kappa^2\vec{B}^2}{\hbar^2\alpha^2}, \delta_7 = \frac{\kappa^2\vec{B}\Phi_{AB}}{\hbar^2\alpha\pi}, \delta_8 = (m+\tau)^2 - \frac{1}{4} \qquad (21)$$

and for mathematical simplicity and convenience Equation (21) becomes:

$$\frac{d^2\chi_{nm}(r)}{ds^2} + \frac{(1-s)}{s(1-s)}\frac{d\chi_{nm}(r)}{ds} + \frac{1}{s^2(1-s)^2}\begin{bmatrix} -(\varepsilon_{nm} + \delta_3 + \delta_6)s^2 + (2\varepsilon_{nm} - \delta_1 + \delta_3 - \delta_4 + \delta_5 - \delta_7) \\ -(\varepsilon_{nm} - \delta_1 + \delta_2 + \delta_8) \end{bmatrix}\chi_{nm}(r) = 0 \qquad (22)$$

Therefore, comparing Equation (22) with the ENU method of Equation (2), then we have the following polynomials of 1st and 2nd degree as:

$$\tilde{\tau}_e(s) = 1 - s \tag{23}$$

$$\sigma_e(s) = s(1-s) \tag{24}$$

$$\tilde{\sigma}_e(s) = -(\varepsilon_{nm} + \delta_3 + \delta_6)s^2 + (2\varepsilon_{nm} - \delta_1 + \delta_3 - \delta_4 + \delta_5 - \delta_7) - (\varepsilon_{nm} - \delta_1 + \delta_2 + \delta_8) \tag{25}$$

Substituting Eqs. (23) - (25) into Equation (10), we obtain $\pi_e(s)$ to be

$$\pi_e(s) = -\frac{s}{2} \pm \sqrt{\begin{array}{l} -Ps^3 + \left(\frac{1}{4} + \varepsilon_{nm} + \delta_3 + \delta_6 + P - Q\right)s^2 - (2\varepsilon_{nm} - \delta_1 + \delta_3 - \delta_4 + \delta_5 - \delta_7 - Q)s \\ +(\varepsilon_{nm} - \delta_1 + \delta_2 + \delta_8) \end{array}} \tag{26}$$

The function $G(s) = Ps + Q$is chosen such as the function under the root has the form: $(A + Bs + Cs^2)^2$, i.e.,

$$\pi_e(s) = -\frac{s}{2} \pm \sqrt{(A + Bs + Cs^2)^2} \tag{27}$$

Then we obtain the following five sets of solutions:

$$C^2 = 0 \tag{28}$$

$$2BC = -P \tag{29}$$

$$B^2 + 2AC = \frac{1}{4} + \varepsilon_{nm} + \delta_3 + \delta_6 + P - Q \tag{30}$$

$$2AB = -2\varepsilon_{nm} + \delta_1 - \delta_3 + \delta_4 - \delta_5 + \delta_7 + Q \tag{31}$$

$$A^2 = \varepsilon_{nm} - \delta_1 + \delta_2 + \delta_8 \tag{32}$$

$$A = \pm\sqrt{\varepsilon_{nm} - \delta_1 + \delta_2 + \delta_8} \tag{33}$$

From which it is clear that $C = 0$ and $P = 0$. Then $G(s) = Q(s)$and adding Eqs. (28) - (31) and (33), we obtain:

$$B = \pm\sqrt{\frac{1}{4} + \delta_2 + \delta_4 - \delta_5 + \delta_6 + \delta_7 + \delta_8} \mp \sqrt{\varepsilon_{nm} - \delta_1 + \delta_2 + \delta_8} \tag{34}$$

and

$$Q = \mp 2(\delta_2 + \delta_8) + \delta_1 + \delta_3 - \delta_4 + \delta_5 - \delta_7 \mp 2\sqrt{\varepsilon_{nm} - \delta_1 + \delta_2 + \delta_8}\sqrt{\frac{1}{4} + \delta_2 + \delta_4 - \delta_5 + \delta_6 + \delta_7 + \delta_8} \tag{35}$$

From the knowledge of ENU method, we choose the negative derivative of $\pi_e(s)$ and $\tau_e(s)$. This is given by:

$$\pi_e^{'}(s)_- = -\frac{1}{2} - B_- \tag{36}$$

and

$$\tau_e^{'}(s)_- = -2 - 2B_- \tag{37}$$

Substituting Equation (36) into Equation (11) with $G(s) = Q_-(s)$ and also Eqs. (37) and (24) into (5), we have:

$$h(s) = Q - \frac{1}{2} - B \tag{38}$$

$$h_n(s) = -n\tau_e^{'}(s) - \frac{n(n-1)}{2}\sigma''(s) \tag{39}$$

Equating Eqs. (39) and (40) gives:

$$h(s) = h_n(s) = G(s) + \pi_e^{'}(s) = -n\tau_e^{'}(s) - \frac{n(n-1)}{2}\sigma''(s) \tag{40}$$

and carrying out some algebra yields the energy eigenvalue equation of the SSKP in the form:

$$\varepsilon_{nm} = \delta_1 - \delta_2 - \delta_8 + \left[\frac{\left(n + \frac{1}{2} + \sqrt{\frac{1}{4} + \delta_2 + \delta_4 - \delta_5 + \delta_6 + \delta_7 + \delta_8}\right)^2 - \delta_1 + \delta_2 + \delta_3 + \delta_6 - \delta_8}{2\left(n + \frac{1}{2} + \sqrt{\frac{1}{4} + \delta_2 + \delta_4 - \delta_5 + \delta_6 + \delta_7 + \delta_8}\right)}\right]^2 \tag{41}$$

Substituting the values of dimensionless parameters of Equation (21) into Equation (41) we obtained the analytical energy equation explicitly as:

$$\begin{aligned} E_{nm} &= 2\alpha^2 D_e b\lambda - 4\alpha D_e a\lambda \\ &+ \frac{\hbar^2\alpha^2}{2\mu}\left[(m+\tau)^2 - \frac{1}{4}\right] - \frac{\hbar^2\alpha^2}{2\mu}\left[\begin{array}{c} \dfrac{\left(n + \frac{1}{2} + \sqrt{\frac{2\mu D_e b(2\lambda+\gamma)}{\hbar^2} - \frac{2m\kappa\vec{B}}{\hbar\alpha} + \frac{\kappa^2\vec{B}^2}{\hbar^2\alpha^2} + \frac{\kappa^2\vec{B}\Phi_{AB}}{\hbar^2\alpha\pi} + (m+\tau)^2}\right)}{2} \\ + \dfrac{\frac{4\mu D_e a(\gamma-2\lambda)}{\hbar^2\alpha} + \frac{4\mu D_e b\lambda}{\hbar^2} + \frac{\kappa^2\vec{B}^2}{\hbar^2\alpha^2} - \left[(m+\tau)^2 - \frac{1}{4}\right]}{2\left(n + \frac{1}{2} + \sqrt{\frac{2\mu D_e b(2\lambda+\gamma)}{\hbar^2} - \frac{2m\kappa\vec{B}}{\hbar\alpha} + \frac{\kappa^2\vec{B}^2}{\hbar^2\alpha^2} + \frac{\kappa^2\vec{B}\Phi_{AB}}{\hbar^2\alpha\pi} + (m+\tau)^2}\right)} \end{array}\right]^2 \end{aligned} \tag{42}$$

To the best of our knowledge, this result is new and this makes the research work novel.

Since the result obtained in Equation (42) is new and there is no available literature with which to compare this study with, we therefore, investigate the special case by carrying out an appropriate adjustment to the SSKP parameters which reduced to the standard Kratzer potential and the screened Kratzer potential.

Now setting the shifted parameters $\lambda = 0, \gamma = 1$ and $\alpha \to 0$ of equation (1) reduces to Kratzer potential given as:

$$V(r) = -2D_e\left(\frac{a}{r} - \frac{b}{2r^2}\right) \tag{43}$$

Its corresponding energy eigenvalue is obtained as:

$$E_{nl} = -2\mu D_e^2 a^2\left[n + \frac{1}{2} + \sqrt{\frac{2\mu D_e b}{\hbar^2} + \ell(\ell+1)}\right]^{-2} \tag{44}$$

Equation (44) is very consistent with the result obtained in Equation (8) and Equation (28) of Bayrak et al. (2007) and (Ikhdair & Sever, 2009).

Now setting the shifted parameters $\lambda = 0$ and $\gamma = 1$ of equation (1) reduces to Screened Kratzer potential given as:

$$V(r) = -2D_e\left(\frac{a}{r} - \frac{b}{2r^2}\right)e^{-\alpha r} \tag{45}$$

and its corresponding energy eigenvalue is obtained as:

$$E_{n\ell} = \frac{\hbar^2\alpha^2\ell(\ell+1)}{2\mu} - \frac{\hbar^2\alpha^2}{2\mu}\left[\frac{\left(n+\frac{1}{2}+\sqrt{\frac{1}{4}+\frac{2\mu D_e b}{\hbar^2}+\ell(\ell+1)}\right)^2 + \frac{4\mu D_e a}{\hbar^2\alpha} - \ell(\ell+1)}{2\left(n+\frac{1}{2}+\sqrt{\frac{1}{4}+\frac{2\mu D_e b}{\hbar^2}+\ell(\ell+1)}\right)}\right]^2 \tag{46}$$

The result obtained in Equation (46) is consistent with the result obtained in Equation (29) of Ikot et al. (2019).

The corresponding wavefunction can be evaluated by substituting $\pi_e(s)_-$ and $\sigma_e(s)_-$ from Equations. (24) and (27) respectively, into Equation (9) and solving the first-order differential equation. This gives:

$$\phi(s) = s^{\sqrt{\varepsilon_{nm}-\delta_1+\delta_2+\delta_8}}(1-s)^{\frac{1}{2}+\sqrt{\frac{1}{4}+\delta_2+\delta_4-\delta_5+\delta_6+\delta_7+\delta_8}} \tag{47}$$

The weight function $\rho(s)$ from Equation (8), can be obtained as:

$$\rho(s) = s^{2\sqrt{\varepsilon_{nm}-\delta_1+\delta_2+\delta_8}}(1-s)^{2\sqrt{\frac{1}{4}+\delta_2+\delta_4-\delta_5+\delta_6+\delta_7+\delta_8}} \tag{48}$$

From the Rodrigues relation of Equation (7), we obtain:

$$\begin{aligned} y_{nm}(s) &= B_{mn}s^{-2\sqrt{\varepsilon_{nm}-\delta_1+\delta_2+\delta_8}}(1-s)^{-2\sqrt{\frac{1}{4}+\delta_2+\delta_4-\delta_5+\delta_6+\delta_7+\delta_8}} \\ &\times \frac{d^n}{ds^n}\left[s^{n+2\sqrt{\varepsilon_{nm}-\delta_1+\delta_2+\delta_8}}(1-s)^{n+2\sqrt{\frac{1}{4}+\delta_2+\delta_4-\delta_5+\delta_6+\delta_7+\delta_8}}\right] \end{aligned} \tag{49}$$

In terms of the Jacobi polynomial, Equation (49) can be written as:

$$y_{nm}(s) = B_{mn}P_n^{\left(2\sqrt{\varepsilon_{nm}-\delta_1+\delta_2+\delta_8},2\sqrt{\frac{1}{4}+\delta_2+\delta_4-\delta_5+\delta_6+\delta_7+\delta_8}\right)}(1-2s) \tag{50}$$

where $P_n^{(\theta,\vartheta)}$ is the Jacobi polynomial.

Substituting $\phi(s)$ and $y_{nm}(s)$ from Eqs. (47) and (50) respectively, into Equation (3), we obtain

$$\psi(s) = B_{mn}s^{2\sqrt{\varepsilon_{nm}-\delta_1+\delta_2+\delta_8}}(1-s)^G P_n^{\left(2\sqrt{\varepsilon_{nm}-\delta_1+\delta_2+\delta_8},2G-1\right)}(1-2s) \tag{51}$$

where

$$G = \frac{1}{2} + \sqrt{\frac{1}{4} + \delta_2 + \delta_4 - \delta_5 + \delta_6 + \delta_7 + \delta_8} \tag{52}$$

and B_{mn} is the normalization constant.

From the definition of the Jacobi polynomials (Abramowitz & Stegun, 1964), $P_n^{(\theta,\vartheta)}$ is defined as

$$P_n^{(\theta,\vartheta)}(\omega) = \frac{\Gamma(n+\theta+1)}{n!\Gamma(\theta+1)}\ {}_2F_1\left(-n, \theta+\vartheta+n+1, \theta+1; \frac{1-\omega}{2}\right) \tag{53}$$

In terms of hypergeometric polynomials, Equation (51) which is a total wavefunction can be written as

$$\begin{aligned} \psi(s) &= B_{nm}s^{\sqrt{\varepsilon_{nm}-\delta_1+\delta_2+\delta_8}}(1-s)^G \frac{\Gamma\left(n+2\sqrt{\varepsilon_{nm}-\delta_1+\delta_2+\delta_8}+1\right)}{n!\,\Gamma\left(2\sqrt{\varepsilon_{nm}-\delta_1+\delta_2+\delta_8}+1\right)}\ {}_2F_1 \\ &\left(-n, 2\sqrt{\varepsilon_{nm}-\delta_1+\delta_2+\delta_8}+2G+n, 2\sqrt{\varepsilon_{nm}-\delta_1+\delta_2+\delta_8}+1; s\right) \end{aligned} \tag{54}$$

In order to find the normalization constant, we write the radial wavefunction as

$$|\psi(s)|^2 = B_{nm}^2 s^{2\sqrt{\varepsilon_{nm}-\delta_1+\delta_2+\delta_8}}(1-s)^{2G}\left[P_n^{\left(2\sqrt{\varepsilon_{nm}-\delta_1+\delta_2+\delta_8},2G-1\right)}(1-2s)\right]^2, \quad s = e^{-\alpha r} \tag{55}$$

Equation (55) also represent the probability density $\rho(s)$. Effecting the normalization condition, given by

$$\int_0^{\infty}|\psi(s)|^2dr = 1 \tag{56}$$

we have that

$$-\frac{B_{nm}^2}{\alpha}\int_1^0 s^{2\sqrt{\varepsilon_{nm}-\delta_1+\delta_2+\delta_8}}(1-s)^{2G}\left[P_n^{\left(2\sqrt{\varepsilon_{nm}-\delta_1+\delta_2+\delta_8},2G-1\right)}(1-2s)\right]^2\frac{ds}{s} = 1,\ s = e^{-\alpha r} \tag{57}$$

Carrying out a coordinate transformation as $z = 1 - 2s$, Equation (57) becomes:

$$\frac{B_{nm}^2}{2\alpha}\int_{-1}^1\left(\frac{1-z}{2}\right)^{2\sqrt{\varepsilon_{nm}-\delta_1+\delta_2+\delta_8}}\left(\frac{1+z}{2}\right)^{2G}\left[P_n^{\left(2\sqrt{\varepsilon_{nm}-\delta_1+\delta_2+\delta_8},2G-1\right)}(z)\right]^2dz = 1 \tag{58}$$

Using the integral standard (Gradshteyn and Ryzhik, 2007)

$$\int_{-1}^1\left(\frac{1-t}{2}\right)^a\left(\frac{1+t}{2}\right)^b\left[P_n^{(a,b-1)}(t)\right]^2dt = \frac{2^{a+b+1}\Gamma(a+n+1)\Gamma(b+n+1)}{n!\Gamma(a+b+n+1)\Gamma(a+b+2n+1)} \tag{59}$$

We have the normalization constant in Equation (58) as:

$$B_{nm} = \sqrt{\frac{2\alpha(n!)\Gamma\left(1+n+2G+2\sqrt{\varepsilon_{nm}-\delta_1+\delta_2+\delta_8}\right)\Gamma(1+2n+2G)+2\sqrt{\varepsilon_{nm}-\delta_1+\delta_2+\delta_8}}{2^{\left(1+2G+2\sqrt{\varepsilon_{nm}-\delta_1+\delta_2+\delta_8}\right)}\Gamma\left(1+n+2\sqrt{\varepsilon_{nm}-\delta_1+\delta_2+\delta_8}\right)\Gamma(1+n+2G)}} \tag{60}$$

RESULTS AND DISCUSSION

In this section, we use the energy spectrum of equation (42) for this research work to study the numerical computation of energy spectra and graphical results for four diatomic molecules H_2, LiH, HCl and CO. Table 1 shows the spectroscopic parameters for the four diatomic molecules as our input. Tables 2 – 13 shows the energy spectra for SSKP model for four diatomic molecules H_2, LiH, HCl and CO in the presence of magnetic field, $\vec{B} = 0.0001$T, AB-flux field $\Phi_{\text{AB}} = 0.0001T$ for 1 Gauss and shifting parameters $(\lambda,\gamma) = (0,0)$, $(\lambda,\gamma) = (1,0)$and $(\lambda,\gamma) = (0,1)$ with distinct values of the vibrational quantum number $0 \le n \le 3$ and magnetic quantum number $-1 \le m \le 1$ for constant values of the other parameters $e = c = \hbar = \phi = 1$in natural units computed using Equation (42). It is worthy to mention in this research work that the following conversions have been adopted throughout our computations: $\hbar c = 1973.269$eVÅand $1a.m.u = 931.494028$MeVc^{-2}.

Table 1: Spectroscopic Parameters for the Diatomic Molecule Systems Nasser et al. (2007)

Molecules	$D_e(eV)$	$r_e(\mathring{A})$	$\mu(a.m.u.)$	$\alpha(\mathring{A}^{-1})$
H_2	4.7446	0.7416	0.50391	1.9426
LiH	2.5152672118	1.5956	0.8801221	1.1280
HCl	4.619030905	1.2746	0.9801045	1.8677
CO	11.2256	1.1283	6.8606719	2.2994

Table 2: Numerical Energy Eigenvalues for the Shifted Screened Kratzer Potential model for H_2 diatomic molecule for $(\lambda,\gamma) = (0,0)$.

m	n	$B = 0$, $\Phi_{\text{AB}} = 0$	$B = 0.0001$, $\Phi_{\text{AB}} = 0$	$B = 0$, $\Phi_{\text{AB}} = 0.0001$	$B = 0.0001$, $\Phi_{\text{AB}} = 0.0001$
-1	0	0.007826283130	−0.9386111768	0.007823152782	−0.9817350233
	1	−0.007200180490	−0.9396111798	−0.007202759860	−1.034292724
	2	−0.03050653224	−0.9667571448	−0.03050840304	−1.101352595
	3	−0.06174067810	−1.013310073	−0.06174179870	−1.180895945
0	0	−0.007826283140	−0.9699763456	−0.007826282982	−1.048398762
	1	−0.01478297926	−0.9957247046	−0.01478413849	−1.111541465
	2	−0.03036597858	−1.041266037	−0.03036793181	−1.187732205
	3	−0.05382566158	−1.102567380	−0.05382839945	−1.275478095
1	0	0.007826283130	−0.9667571448	0.007829413810	−1.070819448
	1	−0.007200180490	−1.013310073	−0.007197600770	−1.145178030
	2	−0.03050653224	−1.075367096	−0.03050466103	−1.231209334
	3	−0.06174067810	−1.150540997	−0.06173955707	−1.327873264

Table 3: Numerical Energy Eigenvalues of the Shifted Screened Kratzer Potential model for LiH diatomic molecule for $(\boldsymbol{\lambda}, \boldsymbol{\gamma}) = (\mathbf{0}, \mathbf{0})$.

$\boldsymbol{m}$	$\boldsymbol{n}$	$\boldsymbol{B} = \mathbf{0}$, $\boldsymbol{\Phi}_{\mathbf{AB}} = \mathbf{0}$	$\boldsymbol{B} = \mathbf{0.0001}$, $\boldsymbol{\Phi}_{\mathbf{AB}} = \mathbf{0}$	$\boldsymbol{B} = \mathbf{0}$, $\boldsymbol{\Phi}_{\mathbf{AB}} = \mathbf{0.0001}$	$\boldsymbol{B} = \mathbf{0.0001}$, $\boldsymbol{\Phi}_{\mathbf{AB}} = \mathbf{0.0001}$
-1	0	0.001510834999	−0.5450611265	0.001510230696	−0.5540913729
	1	−0.001389968201	−0.5451732235	−0.001390466136	−0.5656479434
	2	−0.005889173162	−0.5507152100	−0.005889534310	−0.5807971880
	3	−0.01191880944	−0.5607374000	−0.01191902576	−0.5990982298
0	0	−0.001510834999	−0.5511084760	−0.001510834969	−0.5692328971
	1	−0.002853799444	−0.5564694055	−0.002854023232	−0.5837532354
	2	−0.005862039794	−0.5663434580	−0.005862416864	−0.6015027559
	3	−0.01039084479	−0.5800445875	−0.01039137332	−0.6221331900
1	0	0.001510834999	−0.5507152100	0.001511439364	−0.5761343545
	1	−0.001389968201	−0.5607374000	−0.001389470195	−0.5935739403
	2	−0.005889173162	−0.5745612690	−0.005888811932	−0.6139202155
	3	−0.01191880944	−0.5916915895	−0.01191859304	−0.6369021474

Table 4: Numerical Energy Eigenvalues of the Shifted Screened Kratzer Potential model for HCl diatomic molecule $(\boldsymbol{\lambda}, \boldsymbol{\gamma}) = (\mathbf{0}, \mathbf{0})$.

$\boldsymbol{m}$	$\boldsymbol{n}$	$\boldsymbol{B} = \mathbf{0}$, $\boldsymbol{\Phi}_{\mathbf{AB}} = \mathbf{0}$	$\boldsymbol{B} = \mathbf{0.0001}$, $\boldsymbol{\Phi}_{\mathbf{AB}} = \mathbf{0}$	$\boldsymbol{B} = \mathbf{0}$, $\boldsymbol{\Phi}_{\mathbf{AB}} = \mathbf{0.0001}$	$\boldsymbol{B} = \mathbf{0.0001}$, $\boldsymbol{\Phi}_{\mathbf{AB}} = \mathbf{0.0001}$
-1	0	0.003719491906	−0.4833672175	0.003718004181	−0.5040044184
	1	−0.003421932555	−0.4838241519	−0.003423158420	−0.5292564258
	2	−0.01449842764	−0.4967893891	−0.01449931676	−0.5615365123
	3	−0.02934265838	−0.5191201416	−0.02934319096	−0.5998674527
0	0	−0.003719491908	−0.4982716219	−0.003719491834	−0.5361136185
	1	−0.007025706934	−0.5105898860	−0.007026257875	−0.5665516267
	2	−0.01443162859	−0.5324473545	−0.01443255689	−0.6033046445
	3	−0.02558099536	−0.5619330100	−0.02558229656	−0.6456473010
1	0	0.003719491906	−0.4967893891	0.003720979781	−0.5472252375
	1	−0.003421932555	−0.5191201416	−0.003420706520	−0.5831150517
	2	−0.01449842764	−0.5489624271	−0.01449753834	−0.6246520800
	3	−0.02934265838	−0.5851651896	−0.02934212562	−0.6713263233

Table 5: Numerical Energy Eigenvalues of the Shifted Screened Kratzer Potential model for CO diatomic molecule for $(\boldsymbol{\lambda}, \boldsymbol{\gamma}) = (\mathbf{0}, \mathbf{0})$.

$\boldsymbol{m}$	$\boldsymbol{n}$	$\boldsymbol{B} = \mathbf{0}$, $\boldsymbol{\Phi}_{\mathbf{AB}} = \mathbf{0}$	$\boldsymbol{B} = \mathbf{0.0001}$, $\boldsymbol{\Phi}_{\mathbf{AB}} = \mathbf{0}$	$\boldsymbol{B} = \mathbf{0}$, $\boldsymbol{\Phi}_{\mathbf{AB}} = \mathbf{0.0001}$	$\boldsymbol{B} = \mathbf{0.0001}$, $\boldsymbol{\Phi}_{\mathbf{AB}} = \mathbf{0.0001}$
-1	0	0.0008053861691	−0.06833843935	0.0008050640312	−0.07263830140
	1	−0.0007409552770	−0.06846024685	−0.0007412207140	−0.07778662562
	2	−0.003139362416	−0.07119015800	−0.003139554938	−0.08430588777
	3	−0.006353602006	−0.07578226600	−0.006353717324	−0.09200772827
0	0	−0.0008053861696	−0.07156854413	−0.0008053861535	−0.07909844946
	1	−0.001521284988	−0.07413832288	−0.001521404283	−0.08519751033
	2	−0.003124898339	−0.07862006498	−0.003125099343	−0.09254021322
	3	−0.005539084475	−0.08459856998	−0.005539366224	−0.1009889628
1	0	0.0008053861691	−0.07119015800	0.0008057083402	−0.08098905092
	1	−0.0007409552770	−0.07578226600	−0.0007406898030	−0.08813593954
	2	−0.003139362416	−0.08184004350	−0.003139169855	−0.09639898133

3	−0.006353602006	−0.08913689000	−0.006353486650	−0.1056862327

Table 6: Numerical Energy Eigenvalues of the Shifted Screened Kratzer Potential model for H_2 diatomic molecule for $(\lambda, \gamma) = (1, 0)$.

m	n	$B = 0$, $\Phi_{AB} = 0$	$B = 0.0001$, $\Phi_{AB} = 0$	$B = 0$, $\Phi_{AB} = 0.0001$	$B = 0.0001$, $\Phi_{AB} = 0.0001$
-1	0	−9.596500041	−10.06789445	−9.596503464	−10.20325931
	1	−9.843452524	−10.33038152	−9.843455947	−10.47096724
	2	−10.10123885	−10.60284460	−10.10124227	−10.74853614
	3	−10.36955443	−10.88506941	−10.36955785	−11.03576582
0	0	−9.613621172	−10.14117768	−9.613621171	−10.27691658
	1	−9.860576362	−10.40582984	−9.860576361	−10.54673151
	2	−10.11835768	−10.68040254	−10.11835768	−10.82635610
	3	−10.38666122	−10.96468809	−10.38666122	−11.11559615
1	0	−9.596500041	−10.17972230	−9.596496618	−10.31572936
	1	−9.843452524	−10.44653463	−9.843449097	−10.58765141
	2	−10.10123885	−10.72322721	−10.10123542	−10.86934624
	3	−10.36955443	−11.00959749	−10.36955101	−11.16062429

Table 7: Numerical Energy Eigenvalues of the Shifted Screened Kratzer Potential model for LiH diatomic molecule for $(\lambda, \gamma) = (1, 0)$.

m	n	$B = 0$, $\Phi_{AB} = 0$	$B = 0.0001$, $\Phi_{AB} = 0$	$B = 0$, $\Phi_{AB} = 0.0001$	$B = 0.0001$, $\Phi_{AB} = 0.0001$
-1	0	−5.082996304	−5.448840002	−5.082997034	−5.498169177
	1	−5.194148314	−5.562276436	−5.194149040	−5.612275690
	2	−5.306862990	−5.677247564	−5.306863713	−5.727916354
	3	−5.421137652	−5.793752166	−5.421138373	−5.845089986
0	0	−5.086611601	−5.472890492	−5.086611601	−5.522221959
	1	−5.197757360	−5.586597007	−5.197757360	−5.636596852
	2	−5.310465629	−5.701837881	−5.310465629	−5.752505575
	3	−5.424733737	−5.818611919	−5.424733737	−5.869946965
1	0	−5.082996304	−5.489613088	−5.082995583	−5.538944373
	1	−5.194148314	−5.603603689	−5.194147595	−5.653601642
	2	−5.306862990	−5.719128534	−5.306862270	−5.769792629
	3	−5.421137652	−5.836186430	−5.421136933	−5.887516178

Table 8: Numerical Energy Eigenvalues of the Shifted Screened Kratzer Potential model for HCl diatomic molecule for $(\lambda, \gamma) = (1, 0)$.

m	n	$B = 0$, $\Phi_{AB} = 0$	$B = 0.0001$, $\Phi_{AB} = 0$	$B = 0$, $\Phi_{AB} = 0.0001$	$B = 0.0001$, $\Phi_{AB} = 0.0001$
-1	0	−9.383605322	−9.761011942	−9.383607330	−9.832687736
	1	−9.691693672	−10.06936370	−9.691695650	−10.14197815
	2	−10.00376679	−10.38172832	−10.00376878	−10.45527826
	3	−10.31981264	−10.69809248	−10.31981461	−10.77257492
0	0	−9.393527066	−9.800586386	−9.393527066	−9.872264967
	1	−9.701577946	−10.10928837	−9.701577946	−10.18190443
	2	−10.01361415	−10.42200246	−10.01361415	−10.49555285
	3	−10.32962359	−10.73871542	−10.32962359	−10.81319714
	0	−-9.383605322	−9.820253822	−9.383603334	−9.891942947

1	1	−9.691693672	−10.12938172	−9.691691694	−10.20200673
	2	−10.00376679	−10.44251980	−10.00376483	−10.51607761
	3	−10.31981264	−10.75965500	−10.31981067	−10.83414262

Table 9: Numerical Energy Eigenvalues of the Shifted Screened Kratzer Potential model for CO diatomic molecule for $(\lambda, \gamma) = (1, 0)$.

m	n	$B = 0$, $\Phi_{AB} = 0$	$B = 0.0001$, $\Phi_{AB} = 0$	$B = 0$, $\Phi_{AB} = 0.0001$	$B = 0.0001$, $\Phi_{AB} = 0.0001$
-1	0	−22.56661747	−22.62152817	−22.56661804	−22.63375922
	1	−22.80128887	−22.85619362	−22.80128934	−22.86847330
	2	−23.03688992	−23.09178927	−23.03689044	−23.10411747
	3	−23.27341917	−23.32831347	−23.27341964	−23.34069012
0	0	−22.56883529	−22.62880099	−22.56883529	−22.64103166
	1	−22.80350394	−22.86348384	−22.80350394	−22.87576311
	2	−23.03910234	−23.09909684	−23.03910234	−23.11142463
	3	−23.27562889	−23.33563839	−23.27562889	−23.34801462
1	0	−22.56661747	−22.63163757	−22.56661705	−22.64386809
	1	−22.80128887	−22.86634322	−22.80128845	−22.87862234
	2	−23.03688992	−23.10197897	−23.03688950	−23.11430661
	3	−23.27341917	−23.33854317	−23.27341875	−23.35091930

Table 10: Numerical Energy Eigenvalues of the Shifted Screened Kratzer Potential model for H_2 diatomic molecule for $(\lambda, \gamma) = (0, 1)$.

m	n	$B = 0$, $\Phi_{AB} = 0$	$B = 0.0001$, $\Phi_{AB} = 0$	$B = 0$, $\Phi_{AB} = 0.0001$	$B = 0.0001$, $\Phi_{AB} = 0.0001$
-1	0	−13.92852356	−14.90552170	−13.92853095	−14.80318111
	1	−13.79744424	−14.76955924	−13.79745129	−14.69916836
	2	−13.70997642	−14.67733523	−13.70998317	−14.63536931
	3	−13.66120412	−14.62406285	−13.66121059	−14.60756785
0	0	−13.96553773	−14.89636325	−13.96553773	−14.80369115
	1	−13.83276202	−14.77247476	−13.83276202	−14.71044565
	2	−13.74378766	−14.69096909	−13.74378766	−14.65625612
	3	−13.69366920	−14.64728264	−13.69366920	−14.63709291
1	0	−13.92852356	−14.81901078	−13.92851616	−14.73770638
	1	−13.79744424	−14.70971294	−13.79743716	−14.65756134
	2	−13.70997642	−14.64120144	−13.70996966	−14.61509701
	3	−13.66120412	−14.60916837	−13.66119760	−14.60649894

Table 11: Numerical Energy Eigenvalues of the Shifted Screened Kratzer Potential model for LiH diatomic molecule for $(\lambda, \gamma) = (0, 1)$.

m	n	$B = 0$, $\Phi_{AB} = 0$	$B = 0.0001$, $\Phi_{AB} = 0$	$B = 0$, $\Phi_{AB} = 0.0001$	$B = 0.0001$, $\Phi_{AB} = 0.0001$
-1	0	−9.066226693	−9.617656938	−9.066227952	−9.609250988
	1	−9.054798793	−9.605130588	−9.054800042	−9.600744258
	2	−9.049872718	−9.599152553	−9.049873942	−9.598568979
	3	−9.051091613	−9.599371863	−9.051092802	−9.602392816
0	0	−9.072548922	−9.620168387	−9.072548922	−9.612748454
	1	−9.060995512	−9.609204822	−9.060995512	−9.605734619
	2	−9.055950862	−9.604704657	−9.055950862	−9.604972813
	3	−9.057057542	−9.606324287	−9.057057542	−9.610137520

	0	−9.066226693	−9.610522408	−9.066225433	−9.604209195
	1	−9.054798793	−9.601331598	−9.054797568	−9.598891228
1	2	−9.049872718	−9.598508823	−9.049871503	−9.599735905
	3	−9.051091613	−9.601718628	−9.051090423	−9.606425249

Table 12: Numerical Energy Eigenvalues of the Shifted Screened Kratzer Potential model for HCl diatomic molecule for $(\boldsymbol{\lambda}, \boldsymbol{\gamma}) = (\mathbf{0}, \mathbf{1})$.

$\boldsymbol{m}$	$\boldsymbol{n}$	$\boldsymbol{B} = \mathbf{0}$, $\boldsymbol{\Phi}_{\text{AB}} = \mathbf{0}$	$\boldsymbol{B} = \mathbf{0.0001}$, $\boldsymbol{\Phi}_{\text{AB}} = \mathbf{0}$	$\boldsymbol{B} = \mathbf{0}$, $\boldsymbol{\Phi}_{\text{AB}} = \mathbf{0.0001}$	$\boldsymbol{B} = \mathbf{0.0001}$, $\boldsymbol{\Phi}_{\text{AB}} = \mathbf{0.0001}$
	0	−22.18291952	−22.66300290	−22.18292225	−22.68623410
	1	−22.25931120	−22.73743048	−22.25931390	−22.76431820
-1	2	−22.34654525	−22.82282136	−22.34654791	−22.85321208
	3	−22.44417185	−22.91872100	−22.44417447	−22.95247318
	0	−22.19655419	−22.68612467	−22.19655419	−22.70974438
	1	−22.27275225	−22.76187959	−22.27275225	−22.78912947
0	2	−22.35980148	−22.84854239	−22.35980148	−22.87927078
	3	−22.45725139	−22.94566302	−22.45725139	−22.97972994
	0	−22.18291952	−22.68212420	−22.18291681	−22.70624805
	1	−22.25931120	−22.75957936	−22.25930854	−22.78730067
1	2	−22.34654525	−22.84787060	−22.34654263	−22.87903986
	3	−22.44417185	−22.94655324	−22.44416925	−22.98103258

Table 13: Numerical Energy Eigenvalues of the Shifted Screened Kratzer Potential model for CO diatomic molecule for $(\boldsymbol{\lambda}, \boldsymbol{\gamma}) = (\mathbf{0}, \mathbf{1})$.

$\boldsymbol{m}$	$\boldsymbol{n}$	$\boldsymbol{B} = \mathbf{0}$, $\boldsymbol{\Phi}_{\text{AB}} = \mathbf{0}$	$\boldsymbol{B} = \mathbf{0.0001}$, $\boldsymbol{\Phi}_{\text{AB}} = \mathbf{0}$	$\boldsymbol{B} = \mathbf{0}$, $\boldsymbol{\Phi}_{\text{AB}} = \mathbf{0.0001}$	$\boldsymbol{B} = \mathbf{0.0001}$, $\boldsymbol{\Phi}_{\text{AB}} = \mathbf{0.0001}$
	0	−59.27281877	−59.34010602	−59.27281934	−59.34541414
	1	−59.34582867	−59.41302472	−59.34582924	−59.41849636
-1	2	−59.42104067	−59.48814697	−59.42104124	−59.49378032
	3	−59.49842937	−59.56544752	−59.49842994	−59.57124073
	0	−59.27568694	−59.34516674	−59.27568694	−59.35047784
	1	−59.34868609	−59.41814229	−59.34868609	−59.42361685
0	2	−59.42388744	−59.49332079	−59.42388744	−59.49895696
	3	−59.50126569	−59.57067694	−59.50126569	−59.57647288
	0	−59.27281877	−59.34449232	−59.27281820	−59.34980782
	1	−59.34582867	−59.41754617	−59.34582810	−59.42302510
1	2	−59.42104067	−59.49280212	−59.42104010	−59.49844256
	3	−59.49842937	−59.57023482	−59.49842880	−59.57603493

Table 14: Comparison of the Numerical Energy levels corresponding to the Kratzer Potential for the various $\boldsymbol{n}$and $\boldsymbol{\ell}$quantum number for the diatomic molecules $\boldsymbol{I_2}$and $\boldsymbol{O_2}$

$\boldsymbol{n}$	$\boldsymbol{\ell}$	$\boldsymbol{I_2}$ [EQR] Ikhdair & Sever (2009)	$\boldsymbol{I_2}$ [AIM] Bayrak et al. (2006)	$\boldsymbol{I_2}$ [ENU(Present)]	$\boldsymbol{O_2}$ [EQR] Ikhdair & Sever (2009)	$\boldsymbol{O_2}$ [AIM] Bayrak et al. (2006)	$\boldsymbol{O_2}$ [ENU(Present)]
0	0	−1.579082576525	−1.579082577	−1.579082564	−5.126358620071	−5.126358625	−5.126358491
1	0	−1.573687150333	−1.573687151	−1.573687115	−5.066641146718	−5.066641151	−5.066640767
	1	−1.573677924919	−1.573677925	−1.573677890	−5.066292321402	−5.066292323	−5.066291937
	0	−1.568319329698	−1.568319330	−1.568319272	−5.007961110233	−5.007961116	−5.007960488

2	1	−1.568310151445	−1.568310152	−1.568310094	−5.007618327191	−5.007618329	−5.007617702
	2	−1.568291795200	−1.568291796	−1.568291737	−5.006932902380	−5.006932904	−5.006932273
3	0	−1.562978926616	−1.562978927	−1.562978847	−4.950294618656	−4.950294624	−4.950293763
	1	−1.562969795203	−1.562969796	−1.562969715	−4.949957739138	−4.949957740	−4.949956880
	2	−1.562951532697	−1.562951533	−1.562951452	−4.949284118344	−4.949284119	−4.949283255
	3	−1.562924139740	−1.562924140	−1.562924059	−4.948274032620	−4.948274034	−4.948273159
4	0	−1.557665754681	−1.557665755	−1.557665652	−4.893618463868	−4.893618469	−4.893617383
	1	−1.557656669790	−1.557656670	−1.557656567	−4.893287353086	−4.893287355	−4.893286268
	2	−1.557638500327	−1.557638501	−1.557638398	−4.892625266816	−4.892625268	−4.892624178
	3	−1.557611246928	−1.557611247	−1.557611144	−4.891632475505	−4.891632476	−4.891631377
	4	−1.557574910549	−1.557574911	−1.557574807	−4.890309384483	−4.890309388	−4.890308272
5	0	−1.552379629069	−1.552379630	−1.552379504	−4.837910098245	−4.837910103	−4.837908798
	1	−1.552370590385	−1.552370591	−1.552370466	−4.837584625235	−4.837584627	−4.837583322
	2	−1.552352513333	−1.552352514	−1.552352389	−4.836933811639	−4.836933812	−4.836932505
	3	−1.552325398546	−1.552325399	−1.552325274	−4.835957922172	−4.835957923	−4.835956606
	4	−1.552289246974	−1.552289248	−1.552289121	−4.834657353568	−4.834657357	−4.834656025
	5	−1.552244059882	−1.552244060	−1.552243934	−4.833032634174	−4.833032637	−4.833031292

Table 15: Comparison of the Numerical Energy levels corresponding to the Kratzer Potential for the various $n$and ℓquantum number for the diatomic moleculesNOand CO

n	ℓ	NO [EQR] Ikhdair & Sever (2009)	NO [AIM] Bayrak et al. (2006)	NO [ENU(Present)]	CO [EQR] Ikhdair & Sever (2009)	CO [AIM] Bayrak et al. (2006)	CO [ENU(Present)]
0	0	−8.002659419493	−8.002659417	−8.002659249	−10.794315323	−10.79431532	−10.79431511
1	0	−7.921456840689	−7.921456839	−7.921456327	−10.693839925	−10.69383992	−10.69383928
	1	−7.921043829925	−7.921043834	−7.921043312	−10.693371229	−10.69337123	−10.69337058
2	0	−7.841483958093	−7.841483956	−7.841483114	−10.594760890	−10.59476089	−10.59475984
	1	−7.841077185904	−7.841077188	−7.841076336	−10.594298692	−10.59429869	−10.59429764
	2	−7.840263768523	−7.840263771	−7.840262914	−10.593374417	−10.59337441	−10.59337335
3	0	−7.762716067159	−7.762716066	−7.762714900	−10.497052462	−10.49705246	−10.49705101
	1	−7.762315408528	−7.762315413	−7.762314236	−10.496596643	−10.49659664	−10.49659519
	2	−7.761514215884	−7.761514218	−7.761513040	−10.495685124	−10.49568512	−10.49568366
	3	−7.760312738370	−7.760312744	−7.760311553	−10.494318144	−10.49431814	−10.49431667
4	0	−7.685129080626	−7.685129079	−7.685127601	−10.400689478	−10.40068947	−10.40068763
	1	−7.684734413653	−7.684734417	−7.684732929	−10.400239921	−10.40023992	−10.40023807
	2	−7.683945202003	−7.683945203	−7.683943714	−10.399340924	−10.39934092	−10.39933907
	3	−7.682761690175	−7.682761696	−7.682760193	−10.397992722	−10.39799272	−10.39799086
	4	−7.681184244677	−7.681184246	−7.681182728	−10.396195666	−10.39619567	−10.39619379
5	0	−7.608699510108	−7.608699509	−7.608697729	−10.305647347	−10.30564735	−10.30564512
	1	−7.608310715917	−7.608310719	−7.608308928	−10.305203938	−10.30520394	−10.30520171
	2	−7.607533247563	−7.607533248	−7.607531457	−10.304317236	−10.30431723	−10.30431500
	3	−7.606367345012	−7.606367349	−7.606365545	−10.302987469	−10.30298747	−10.30298523
	4	−7.604813367976	−7.604813368	−7.604811551	−10.301214985	−10.30121499	−10.30121273
	5	−7.602871795644	−7.602871795	−7.602869969	−10.299000242	−10.29900024	−10.29899796

Table 16: Comparison of Numerical Energy Eigenvalues corresponding to the Screened Kratzer Potential for the various $n$and ℓquantum number for the diatomic molecules LiHand HCl

n	ℓ	LiH ENU (Present)	LiH Ikot et al. NU (2019)	HCl ENU (Present)	HCl Ikot et al. NU (2019)
0	0	−9.070968132	−9.070968135	−22.19329052	−22.19329052
1	0	−9.059446117	−9.059446120	−22.26953722	−22.24266011
	1	−9.047056122	−9.047056120	−22.24266012	−22.24266011
2	0	−9.054431115	−9.054431115	−22.35663287	−22.35663288
	1	−9.042278091	−9.042278085	−22.33012522	−22.33012521
	2	−9.017997943	−9.017997940	−22.27714784	−22.27714784
3	0	−9.055565864	−9.055565865	−22.45412719	−22.45412720
	1	−9.043637069	−9.043637070	−22.42797267	−22.42797265
	2	−9.019803986	−9.019803985	−22.37569980	−22.37569979
	3	−8.984115356	−8.984115355	−22.29738072	−22.29738072
4	0	−9.062524471	−9.062524470	−22.56160483	−22.56160484
	1	−9.050808169	−9.050808170	−22.53578825	−22.53578825
	2	−9.027398775	−9.027398770	−22.48418966	−22.48418965
	3	−8.992342454	−8.992342455	−22.40687787	−22.40687787
	4	−8.945707875	−8.945707875	−22.30395550	−22.30395550
5	0	−9.075009168	−9.075009170	−22.67868228	−22.67868230
	1	−9.063494533	−9.063494530	−22.65318951	−22.65318950
	2	−9.040487259	−9.040487255	−22.60223695	−22.60223694
	3	−9.006031117	−9.006031120	−22.52589038	−22.52589037
	4	−8.960191208	−8.960191210	−22.42424781	−22.42424781
	5	−8.903053290	−8.903053285	−22.29743870	−22.29743871

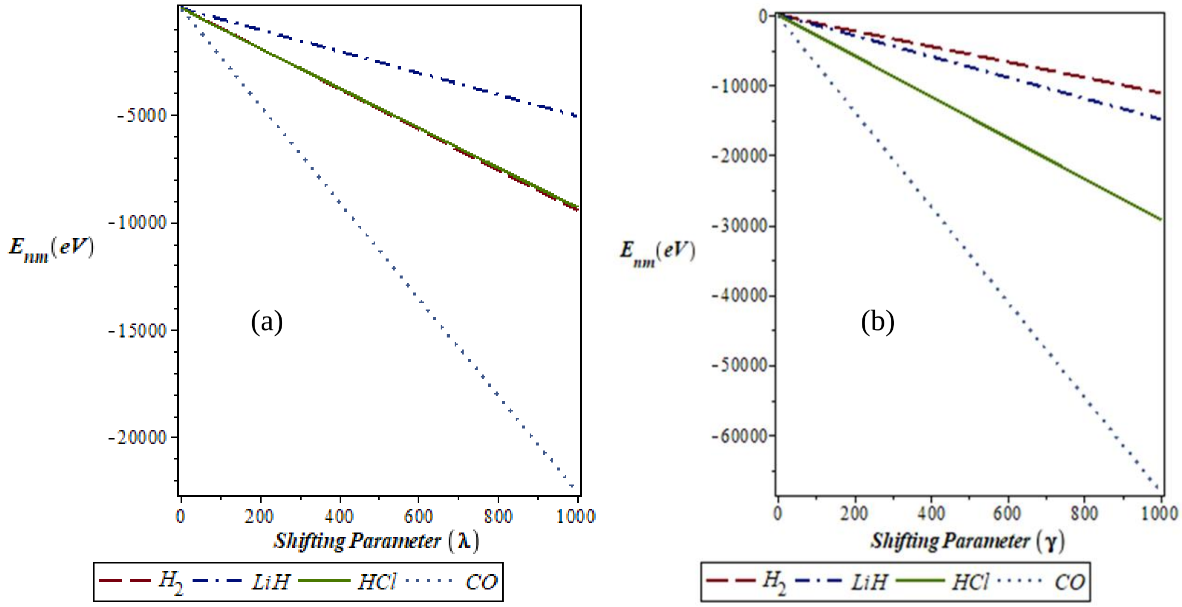

Figure 1: (a) Variation of energy eigenvalues of SSKP with shifting parameter (λ) for different diatomic molecule systems. (b) Variation of energy eigenvalues of SSKP with shifting parameter (γ) for different diatomic molecule systems.

DISCUSSION

From Tables 2 – 5 for $(\lambda,\gamma)=(0,0)$, we observe that when both magnetic and AB-flux fields are absent $\left(\text{i.e}, \vec{B}=\Phi_{\text{AB}}=0\right)$, there exists degeneracies when $m=1$ and $m=-1$ in the energy spectra of the diatomic molecules. By subjecting the systems to the single effect of the magnetic field $\left(\vec{B}\neq 0,\Phi_{\text{AB}}=0\right)$, the numerical energy eigenvalues reduces and degeneracies are removed. However, when only the AB-flux field is applied$\left(\vec{B}=0,\Phi_{\text{AB}}\neq 0\right)$, it takes away degeneracies but yet we still notice some quasi-degeneracies and the numerical energy eigenvalues increases and the system still bounded. The all-inclusive effect of both magnetic and AB-flux fields $\left(\vec{B}=\Phi_{\text{AB}}\neq 0\right)$ are stronger than the single effects and consequently, there is a major shift in the bound state energy of the system. The all-inclusive effect of both fields completely eliminates degeneracies.

From Tables 6 – 9 for $(\lambda,\gamma)=(1,0)$ and for $(\lambda,\gamma)=(0,1)$, we observe that when both magnetic and AB-flux fields are not present $\left(\text{i.e}, \vec{B}=\Phi_{\text{AB}}=0\right)$, degeneracies exist when $m=1$ and $m=-1$ in the energy spectra of the diatomic molecules. On exposing the systems to the magnetic field effect alone $\left(\vec{B}\neq 0,\Phi_{\text{AB}}=0\right)$, the numerical energy eigenvalues reduces and there is removal of degeneracies. In the situation when the AB-flux field alone is functional $\left(\vec{B}=0,\Phi_{\text{AB}}\neq 0\right)$, some quasi-degeneracies are observed and the numerical energy eigenvalues reduces as well. When both magnetic and AB-flux fields are made to be active $\left(\vec{B}=\Phi_{\text{AB}}\neq 0\right)$, is more significant than the singular effects and as a results, there is an ample change in the bound state energy of the system.

More so, it is observed that the effect of shifting parameters greater than zero i.e., $(\lambda=\gamma>0)$ influences the energy eigenvalues of diatomic molecules to becomes strongly negative or bound as it can be seen from the results presented in the tables.

We also plot the energy eigenvalues of Shifted Screened Kratzer Potential as a function of shifting parameters for different diatomic molecules. In Figure 1. (a) Energy eigenvalues of SSKP becomes strongly negative or bound (decreases) with increasing shifting parameter (λ). The same trend is also seen in (b) as the energy eigenvalues of SSKP varies with shifting parameter (γ) for the selected diatomic molecule systems. From both the tables and the graphs, it shows that the energy eigenvalues for some selected diatomic molecules are sensitives to the effects of shifting parameters.

To compared our results with others in the literature, we compute numerically the energy eigenvalues of the special cases for the Kratzer potential and the Screened Kratzer potential for the I_2, O_2, NO and CO diatomic molecules as given in Tables 14, 15 and 16 which are in agreement with the results given in literature.

CONCLUSION

In this research work, we solve the Schrodinger equation with the shifted screened Kratzer potential for some selected diatomic molecules in the presence of magnetic and AB-flux fields using the ENU method. The energy equation and its corresponding wave functions are obtained in a closed form respectively. The numerical results of the energy eigenvalues of the shifted screened Kratzer potential for some selected diatomic molecules for different values of shifting parameters are computed. We also reduced the energy eigenvalues for shifted screened Kratzer potential to that of the standard Kratzer potential and screened Kratzer potential, by adjusting the potential parameters of the shifted screened Kratzer potential. Our numerical results obtained for the standard Kratzer potential and screened Kratzer potential agrees with the results obtained in the literature. We want to note here that, there are no numerical results in the literature for the shifted screened Kratzer potential to compare our work with. Finally, the thermodynamic properties of the considered systems and the theoretic information measure would be in the next edition of this paper.

REFERENCES

Abramowitz, M., & Stegun, I. A. (1964). *Handbook of Mathematical Functions with Formulas, Graphs and Mathematical Tables*. Dover, New York.

Aygun, M., Bayrak, O., Boztosun, I., & Sahin, Y. (2012). The Energy Eigenvalues of the Kratzer Potential in the presence of a magnetic field. *The European Physical Journal D*, 66: 35, 1-5. https://doi.org/10.1140/epjd/e2011-20319-5

Bayrak, O., & Boztosun, I., & Ciftci, H. (2006). Exact Analytical Solutions to the Kratzer Potential by the Asymptotic Iteration Method. *International Journal of Quantum Chemistry*, 107(3), 540-544. https://doi.org/10.1002/qua.21141

Bayrak, O., Kocak, G., & Boztosun, I. (2006). Any l-state Solutions of the Hulthen Potential by the Asymptotic Iteration Method. *Journal of Physics A: Mathematical and General*, 39(37), 11521.

Cetin, A. (2008). A Quantum Pseudodot system with a two-dimensional Pseudoharmonic Potential, *Physics Letters A*, 372(21), 3852-3856.

Edet, C. O., Khordad, R., Ettah, E. B., Aljunid, S. A., Endut, R., Ali, N., Asjad, M., Ushie, P. O., & Ikot, A. N. (2022). Magneto-transport and Thermal Properties of

TiH Diatomic Molecule under the Influence of Magnetic and Aharonov-Bohm (AB) Fields. *Scientific Reports*, 12: 15430, 1-15. https://doi.org/10.1038/s41598-022-19396-x

Eshghi, M., & Mehraban, H. (2017). Study of a 2D charged particle confined by a magnetic and AB flux fields under the radial scalar power potential. *The European Physical Journal Plus*, 132(3), 121. https://doi.org/10.1140/epjp/i2017-11379-x

Falaye, B. J., Ikhdair, S. M., & Hamzavi, M. (2015). Formula method for bound state problems. *Few-Body Systems*, 56(1), 63-78.

Ferkous, N., & Bounames, A. (2013). On the spin-1/2 Aharonov-Bohm problem for modified Poschl-Teller potential, physical regularization and self-adjoint extensions, *The European Journal Plus*, 59(6), 679-683. https://ctp.itp.ac.cn/EN/Y2013/V59/106/679

Ferkous, N., Boultif, A., & Sifour, M. (2019). 2D Pauli Equation with Hulthen Potential in the Presence of Aharonov-Bohm Effect. Communication Theoretical Physics, 134(258), 679-683. https://doi.org/10.1140/epjp/i2019-12608-0

Gradshteyn, I. S., & Ryzhik, I. M. (2012). *Table of Integrals, Series, and Products*, 7th edition, USA.

Greene, R. L. & Aldrich, C. (1976). Variational wave functions for a screened Coulomb potential. Physical. Review. A, 14, 2363–2366. https://doi.org/10.1103/PhysRevA.14.2363

Hassanabadi, H., Lu, L. L., Zarrinkamar, S., Liu, G. H., & Rahimov, H. (2012). Approximate Solutions of Schrodinger Equation under Manning-Rosen Potential in Arbitrary Dimension via SUSYQM. *ACTA PHYSICA POLONICA*, 122(4), 650-654.

Horchani, R., Al-Aamri, H., Al-Kindi, N., Ikot, A. N., Okorie, U. S., Rampho, G. J., & Jelassi, H. (2021). Energy Spectra and Magnetic Properties of Diatomic Molecules in the Presence of Magnetic and AB Fields with the Inversely Quadratic Yukawa Potential. *European Physical Journal D*, 75:36, 1-13. https://doi.org/10.1140/epjd/s10053-021-00038-2

Ibrahim, N., Okorie, U. S., Sulaiman, N., Rampho, G. J., & Ramantswana, M. (2022). Solutions of the Schrodinger Equation of the Shifted Screened Kratzer Potential and its Thermodynamic Functions using the Extended Nikiforov-Uvarov Method. *Frontiers in Physics.* 10:9882279. https://doi.org/10.3389/fphy.2022.988279

Ikot, A. N., Okorie, U. S., Amadi, P. O., Edet, C. O., Rampho, G. J., & Sever, R. (2021). The Nikiforov-Uvarov-Functional Analysis Method: A New Approach for Solving Exponential-Type Potential. *Few Body System*, 62:9, 1-16. https://doi.org/10.1007/s00601-021-01593-5

Ikot, A. N., Edet, C. O., Okorie, U. S., Abdel-Aty, A., H., Ramantswana, M., Rampho, G. J., Alsheri, N. A., Elagan, S. K., & Kaya, S. (2021). Solutions of the 2D Schrodinger Equation and its Thermal Properties for Improved Ultra-Generalized Exponential Hyperbolic Potential. *European Physical Journal Plus*, 136:434, 1-18. https://doi.org/10.1140/epjp/s13360-021-01408-w

Ikot, A. N., Okorie, U. S., Osobonye, G., Amadi, P. O., Edet, C. O., Sithole, M. J., Rampho, G. J., & Sever, R. (2020). Superstatistics of Schrodinger Equation with Pseudo-Harmonic Potential in External Magnetic and Aharonov-Bohm Fields. *Journal of Heliyon*, 6, e03738, 1-7. https://doi.org/10.1016/j.heliyon.2020.e03738

Ikot, A. N., Edet, C. O., Amadi, P. O., Okorie, U. S., Rampho, G. J., & Abdullah, H. Y. (2020). Thermodynamic Properties of Aharonov-Bohm and Magnetic Fields with Screened Kratzer Potential. *European Physical Journal D*, 74:159, 1-13. https://doi.org/10.1140/epjd/e2020-10084-9

Ikhdair, S. M., & Sever, R. (2009). Exact Quantization Rule to the Kratzer-type Potentials: An Application to the Diatomic Molecules. *Journal of Mathematical Chemistry*, 45, 1137-1152. https://doi.org/10.1007/s10910-008-9438-8

Ikhadiar, S. M. (2012). Approximate l-states of the Manning-Rosen Potential by using Nikiforov-Uvarov Method. *International Scholarly Research Network*, 2012, 1-20. https://doi.org/10.5402/2012/201525

Ikhdair, S. M., Hamzavi, M., & Sever, R. (2012). Spectra of Cylindrical Quantum Dots: The Effect of Electrical and Magnetic Fields together with AB Flux field. *Physica B: Condensed Matter*, 407(23), 4523-4529.

Karayer, H., Demirha, D., & Buyukkilic, F. (2015). Extension of Nikiforov-Uvarov Method for the Solution of Heun Equation. *Journal of Mathematical Physics*, 56, 063504, 1-14. https://dx.doi.org/10.1063/1.4922601

Khordad, R. (2010a). Effects of Magnetic Field and Geometrical size on the Interband light Absorption in Quantum Pseudodot System. *Solid State Sciences*, 12(7): 1253-1256. https://doi.org/10.1016/i.solidstatesciences.2010.03.001

Khordad, R. (2010b). Simultaneous Effects of Temperature and Pressure on the Donor Binding Energy in a V-groove Quantum wire. *Superlattices and Microstructures*, 47(3), 422-431.

Nasser, I., Abdelmonem, M. S., Bahlouli, H., & Alhaidar, A. (2007). The Rotating Morse Potential Model for Diatomic Molecules in the Tridiagonal J-Matrix Representation: I. Bound States. *Journal Physics B: Molecular Optical Physics*, 40:4245-57. https://doi.org/10.1088/0953-4075/40/21/011

Nikiforov, A. F., & Uvarov, V. B. (1988). *Special functions of mathematical physics*. Basel: Birkhäuser.

Onyenegecha, C. P., Njoku, I. J., Omame, A., Okereke, C. J., & Onyeocha, E. (2021). Dirac Equation and Thermodynamic Properties with Modified Kratzer Potential. *Heliyon*, 7, e08023, 1-8. https://doi.org/10.1016/j.heliyon.2021.e08023

Purohit, K. R., Parmar, R. H., & Rai, A. K. (2020). Bound State Solution and Thermodynamical Properties of the Screened Cosine Kratzer Potential under Influence of the Magnetic Field and Aharonov-Bohm Flux Field. *Journal Annals of Physics*. https://doi.org/10.1016/j.aop.2020.168335

Rampho, G. J., Ikot, A. N., Edet, C. O., & Okorie, U. S. (2020). Energy Spectra and Thermal Properties of Diatomic Molecules in the Presence of Magnetic and AB Fields with Improved Kratzer Potential. *Molecular Physics*, e1821922. https://doi.org/10.1080/00268976.2020.1821922

Serrano, F. A., Gu, X. Y., & Dong, S. H. (2010). Qiang–Dong proper quantization rule and its applications to exactly solvable quantum systems. *Journal of mathematical physics*, 51(8), 082103.

Tezcan, C., & Sever, R. (2009). A general approach for the exact solution of the Schrödinger Equation. International Journal of Theoretical Physics, 48(2), 337-350.